Cerebral Cortex, 2017; 1–10

doi: 10.1093/cercor/bhx048
Original Article

ORIGINAL ARTICLE

Characterization of White Matter Tracts by Diffusion MR Tractography in Cat and Ferret that Have Similar Gyral Patterns

Avilash Das[1,2,3] and Emi Takahashi[2,3,4]

[1]Medical Sciences in the College of Arts and Sciences, Boston University, Boston, MA, USA, [2]Division of Newborn Medicine, Department of Medicine, Boston Children's Hospital, Harvard Medical School, Boston, MA, USA, [3]Fetal-Neonatal Brain Imaging and Developmental Science Center, Boston Children's Hospital, Harvard Medical School, Boston, MA, USA and [4]Athinoula A. Martinos Center for Biomedical Imaging, Massachusetts General Hospital, Harvard Medical School, Charlestown, MA, USA

Address correspondence to Emi Takahashi. Email: emi@nmr.mgh.harvard.edu, Emi.Takahashi@childrens.harvard.edu

Abstract

The developmental relationships between gyral structures and white matter tracts have long been debated, but it is still difficult to discern whether they influence each other's development or are causally related. To explore this topic, this study used cats and ferrets as models for species that share similar gyral folding patterns and imaged with diffusion magnetic resonance imaging to compare white matter innervations in homologous gyri and other brain regions. Adult cat and ferret brains were analyzed via diffusion spectrum imaging tractography and homologous regions of interest were compared. Although similar genetic lineage and gyral structures would suggest analogous white matter tracts, tractography reveals significantly differing white matter connectivity in both the visual and auditory cortices. Similarities in connectivity were concentrated primarily in the highly conserved cerebellar region. These results correlate well with existing histological and functional studies of both species. Our results indicate that, while the 2 species may share similar gyral structures, they utilize different white matter connectivity; suggesting that while species may share similar gyral structures, they can develop different underlying white matter connectivity.

Key words: brain pathways, cat, diffusion MRI, ferret, gyrus, tractography

Introduction

The neural structures and architecture that underlie brain connectivity and function of different species are a direct result of their unique developmental processes (Markham and Greenough 2004; Hofman 2014). Over many decades, there have been hypotheses and mounting evidence linking fiber maturation and gyral formation (Goldman-Rakic and Rakic 1984; Barbas and Rempel-Clower 1997; Van Essen 1997; Hilgetag and Barbas 2005). However, it is still unclear whether they are causally related or whether they affect each other. To explore a clue for this question, in this study, cats (*Felis catus*) and ferrets (*Mustela putorius furo*) were used as models of 2 species that have very similar gyral folding patterns, and scanned with diffusion magnetic resonance imaging (MRI) to directly compare fiber pathways in the whole brain between the species. Potentially as a result of being genetically similar animals (Cavagna et al. 2000), cats and ferrets also share analogous brain structures. The spatial arrangement of sulci and gyri in the caudal half of the ferret cerebral cortex bears a strong resemblance to the cerebral cortex of a cat (Manger et al. 2004; Foxworthy and Meredith 2011; Mayer et al. 2014).

Because white matter appears homogeneous in conventionally acquired structural MRI images, it is difficult to appreciate

detailed fiber pathways within the white matter. Alternative approaches employing tracer injections are limited to the study of a small number of white matter tracts in a localized area of the brain. As a result of recent technical advances in DTI, we can now study white matter pathways across numerous species on a whole brain scale (Basser et al. 1994, 2000; Pierpaoli et al. 1996; Cellerini et al. 1997; Makris et al. 1997; Conturo et al. 1999; Jones et al. 1999; Mori et al. 1999; Le Bihan et al. 2001; Catani et al. 2002; Takahashi et al. 2007, 2008; Hagmann et al. 2008). While diffusion MRI and histological studies of white matter pathways have been done for both cats (Callaway and Katz 1990; Olavarria and Van Sluyters 1995; Kim et al. 2003) and ferrets (Barnette et al. 2009; Kroenke et al. 2009; Bock et al. 2010), there is a lack of literature examining the similarities and differences between these 2 species. In the current study, we used diffusion MR tractography based on diffusion spectrum imaging (DSI), that is theoretically useful to identify complex fiber directions within an imaging voxel (Wedeen et al. 2008).

Although the similarities of gyral structures and genetics suggest that cat and ferret brains function via similar anatomical connectivity, studies demonstrating differences in visual cortex plasticity suggest differences in white matter pathways in the 2 species (Issa et al. 1999). A more complete characterization of these differences will allow for a better understanding of the development of white matter pathways across species and their relationships with gyral structures. We mapped gyral structures and underlying fiber pathways in both species, and subsequently, using existing literature, explored the functional significance of detected white matter pathways that showed not only resemblance but also significant difference between the species.

Materials and Methods

Specimen Preparation

We performed scans on the brains of 2 young adult cats and 2 young adult ferrets, all of which were at least 70 days old. All animals were obtained from a group involved in vision research at Harvard Medical School (HMS). All procedures were approved by the Massachusetts General Hospital and HMS where the current study was performed. After the cats were euthanized, their brains were perfused with phosphate-buffered saline solution followed by 4% paraformaldehyde, removed from the cranium, and fixed for 1 week in 4% paraformaldehyde solution containing 1 mM gadolinium (Gd-DTPA) MRI contrast agent to reduce the T1 relaxation time while ensuring that enough T2-weighted signal remained. For MR image acquisition, the brains were placed in a Fomblin solution (Fomblin Profludropolyether; Ausimont). Specimens were scanned using a 4.7 T Bruker Biospec MR system at the A.A. Martinos Center for Biomedical Imaging.

Scanning Parameters

The pulse sequence used for image acquisition was a 3D diffusion-weighted spin-echo echo-planar imaging sequence, TR/TE 1000/40 ms, with an imaging matrix of 96 × 96 × 128 pixels. Spatial resolution was 550 × 550 × 600 μm. Anisotropic resolution may produce less spatial resolution along a longer axis compared with that along a shorter axis, which may mean that DSI tractography has less potential to resolve crossing pathways in the direction along the longer axis. However, the voxel size used for the cats and ferrets was nearly isotropic (less than 10% difference) and we believe it did not bias our tractography significantly.

We performed diffusion spectrum encoding as previously described (Wedeen et al. 2005). Briefly, we acquired 515 diffusion-weighted measurements, corresponding to a cubic lattice in q-space contained within the interior of a ball of maximum radius $b_{max} = 4 \times 10^4\,cm^2/s$, with $\delta = 12.0$ ms, $\Delta = 24.2$ ms. The total acquisition time was 18.5 h for each experiment.

Diffusion Data Analyses—DSI Reconstruction

Diffusion Toolkit (http://trackvis.org) was used for DSI reconstruction. DSI reconstruction was based on the Fourier relationship of the attenuated echo signal in q-space $E(q)$ and the average diffusion propagator of the water molecular diffusion $P_s(R)$: $E(q) = \int P_s(R, \Delta)\exp(i2\pi qR)\,dR$, where R is the relative displacement of water molecular diffusion during the diffusion time Δ (Callaghan 1991). Based on this calculation, applying a 3-dimensional (3D) Fourier transform to the echo signal over the q-space would lead us to obtain the 3D probability density function (PDF) and then map the fiber orientations (Lin et al. 2003; Wedeen et al. 2005). The transformation from q-space signal to PDF values was performed voxel-by-voxel. To visualize the PDF, we integrated the second moment of PDF along each radial direction to acquire the orientation distribution function (ODF). In this study, we reconstructed the ODF within each voxel by interpolating along 181 radial directions, as calculated from the vertices of a regular and triangular mesh of the unit sphere surface. By comparing the length of each vector with the lengths of its neighboring vectors, we could obtain the orientational local maxima to represent intravoxel fiber orientations. We normalized all ODFs by the maximum ODF length within each voxel, and calculated fractional anisotropy (FA) from orientation vectors by fitting the data to the usual tensor model.

Diffusion Data Analyses—Tractography

We used Diffusion Toolkit to utilize a streamline algorithm for diffusion tractography. Trajectories were propagated by consistently pursuing the orientation vector of least curvature. We terminated tracking when the angle between 2 consecutive orientation vectors was greater than the given threshold (35°) or when the fibers extended outside the brain surface, by using mask images of the brains created by TrackVis (http://trackvis.org) for each specimen. In many tractography studies, FA values are used to terminate fibers in the gray matter, which in adults has lower FA values than the white matter. However, as one of the objectives of our study was to detect fibers in low FA areas, we used brain mask volumes to terminate tractography fibers without using the FA threshold for tractography. Trajectories were displayed on a 3D workstation of TrackVis. The color coding of fibers is based on a standard RGB code, applied to the vector between the end-points of each fiber.

Diffusion Data Analyses—ROI Placement and Restriction Parameters

Regions of interest (ROIs) were placed within each gyrus as shown in Fig. 1 and were used as a start point for determining similar and differing tracts. In cats, the lateral, suprasylvian, and ectosylvian gyri had 15, 9, and 10 ROI spheres, respectively. In ferret, the 3 homologous gyri contained 11, 8, and 7 ROI spheres, respectively. The reduced number of ROI spheres in

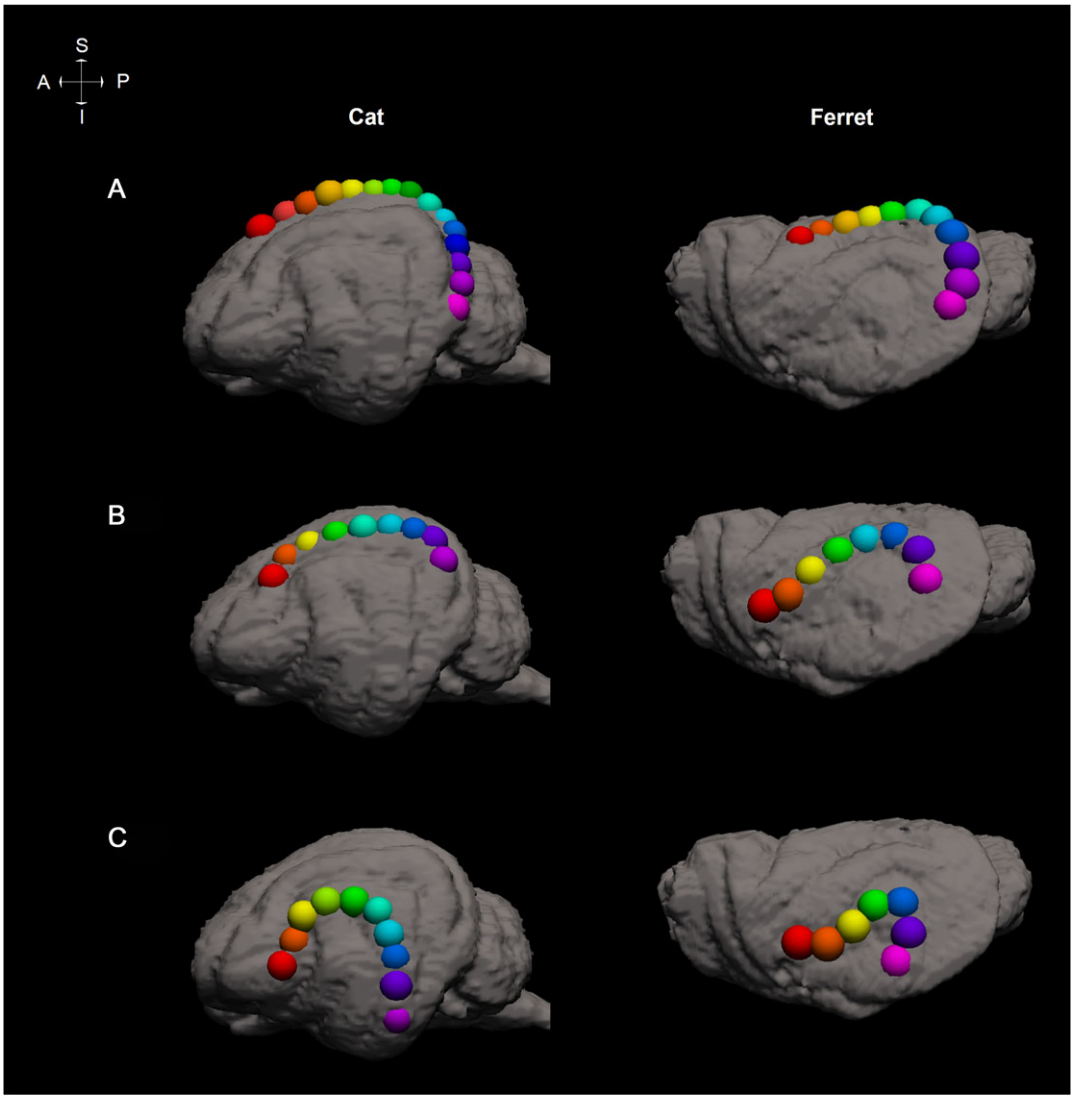

Figure 1. Model detailing placement of ROI spheres in the lateral (*A*), suprasylvian (*B*), and ectosylvian (*C*) gyri for both cats and ferrets. Cat brains are shown on the left and ferrets are shown on the right. The left side of each brain image represents the front of the brain.

ferrets reflects a smaller relative brain size. ROIs were placed into the white matter of each gyrus using brain atlases (Rosenquist 1985; Innocenti et al. 2002).

For Fig. 2, both cingulum and superior longitudinal fasciculus fibers were isolated using ROIs placed at the terminal ends of each structure. For Fig. 3*A* and *B*, ROIs were placed in both the suprasylvian sulcus of area 19 and in area 20 of the visual cortex. In Fig. 3*C–F*, after filtering against cortical fibers in both the lateral and suprasylvian gyri, in order to show U-fiber development clearly, fibers were filtered based on length. In cats, a minimum length threshold of 4.51 mm was utilized. In ferrets, a minimum length threshold of 5.58 mm was used. In Fig. 4*A–D*, tracts were obtained by placing ROIs in both the mid-ectosylvian gyrus (EG) in the primary auditory cortex, A1, and at the lowest most point of the posterior EG. For Fig. 4*E–H*, we set ROIs in the postsylvian gyrus (PG) in cats (EG in ferrets) and again in auditory area A1. Figure 5*A–D* was obtained by placing tractography start points in the primary visual areas and placing additional ROIs in the lateral geniculate nucleus (LGN) of the thalamus. For Fig. 5*E* and *F*, pontocerebellar fibers were isolated by placing ROIs in both the pons and on the lateral surface of the cerebellum. Figure 5*G* and *H* was acquired by placing ROIs in the dentate nucleus and setting a sagittal slice filter to exclude horizontal fibers. In order to clearly show innervations from the dentate nucleus, we set a minimum threshold in both cats and ferrets (about 2 mm). Figure 5*I* and *J* was obtained by combining the existing Fig. 5*G* and *H* and placing additional ROIs in the thalamus. With the exception of Figs 3*C–F* and 5*G* and *H*, no percentage of tracts were omitted or skipped during tractography. All figures generated using ROIs with any-part selectivity filters in TrackVis. For specific ROI placement and relative sizes refer to red circles (spherical ROIs) and orange rectangles (hand drawn ROIs) in Figs 2–5.

Results

Cerebral Fibers

Tractography of the lateral gyrus in cats revealed branching projections from the cingulum bundle that were not found in ferrets. Figure 2*A* and *B* showed the cingulum bundles of both

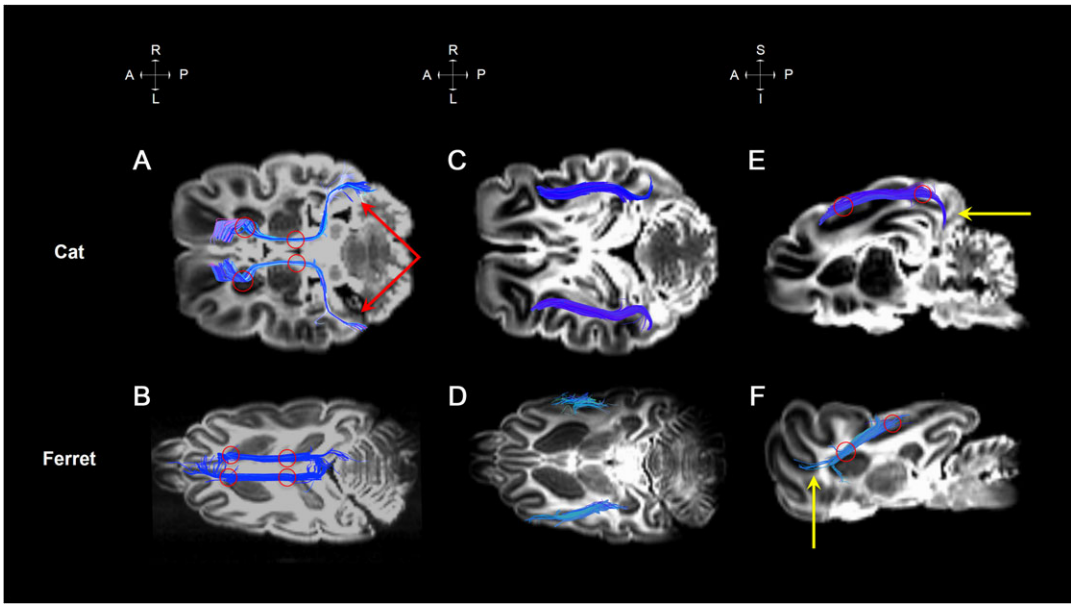

Figure 2. (*A*) and (*B*) show transverse slices of cingulum bundles. (*C*) through (*F*) show transverse and sagittal views of a longitudinal pathway in the suprasylvian gyrus. (*A*), (*C*), and (*E*) show a cat brain while (*B*), (*D*), and (*F*) show a ferret brain. Red arrows in (*A*) show cingulum innervations into the visual cortex in cats. Yellow arrows in (*E*) and (*F*) show the more anterior localization of the longitudinal pathway in the suprasylvian gyrus in ferrets compared with cats. Red circles indicate placement of ROIs.

species in their entirety, highlighting the significantly differing branching and thickness. While the ferret cingulum bundle remained primarily on the midline of the brain, the cat cingulum extends further and terminated in the visual cortex (see red arrows in Fig. 2*A*). In the posterior lateral gyrus of the cat brain, we also detected a set of association fibers connecting areas 19 and 20 of the cat visual cortex (Fig. 3*A*,*B*). When ROIs were placed in homologous visual areas in ferrets no such fibers were observed. Additional tractography of the lateral gyrus revealed U-fiber tracts extending to the suprasylvian gyrus along the length of the gyrus (Fig. 3*C*). Similar seed ROIs placed in ferrets showed no such U-fiber development (see red arrows in Fig. 3*C*,*D*).

ROIs placed in the suprasylvian gyrus of both cats and ferrets showed similar fiber structures. Figure 3*E* and *F* shows U-fiber connections in both species extending down to the EG. Additional fiber similarities in the suprasylvian gyrus include pathways running longitudinally through the suprasylvian gyrus of both cats and ferrets. The cat pathway has terminal points in both the frontal and visual cortices of the brain (Fig. 2*C*), while the ferret pathway begins in the frontal cortex and terminates more anteriorly in the parietal cortex (Fig. 2*D*, see also yellow arrows in Fig. 2*E*,*F*). In addition to its more anterior development, the ferret pathway also is considerably thinner and rougher than its cat counterpart.

Visual cortex fibers imaged in both cats and ferrets included thalamo-cortical bundles between the LGN and the primary visual cortex (Fig. 5, see red circles in Fig. 5*A*,*B* for placement of ROIs). In cats, these tracts extended into both the posterior lateral and suprasylvian gyri while in ferrets they are limited to the lateral gyrus (red arrow in Fig. 5*C* shows suprasylvian innervations in cats). The tracts observed in cats appear more tightly bound and innervate a larger portion of the thalamus (see yellow arrows in Fig. 5*C*,*D*). Tractography of the EG yielded several association fibers in both cat and ferret brains (Fig. 4, see red circles for placement of ROIs). In cats, the pathway shown in Fig. 4*A*–*D* ran vertically through the posterior EG and extends to the primary auditory cortex, A1. An additional branch of the tract reaches auditory areas in the lower PG (Fig. 4*A*,*B*). ROIs placed in homologous locations in ferrets yielded substantially differing tracts (Fig. 4*C*,*D*). As in cats, ferret brains contained a set of fiber tracts along the posterior EG. While the fibers found in cats remained principally in the auditory cortex, the fibers found in ferrets extended into area 21 of the ferret visual cortex (see red arrow in Fig. 4*C*).

The cortico-cortical tracts shown in Fig. 4*E*–*H* were relatively similar in both cat and ferret brains (the difference in color mapping is due to the angled orientation of the EG in relation to the ferret brain). In cats, tracts originate in the anterior auditory field (AAF) and A1 and terminated in the PG, while, in ferrets, tracts originated in the AAF and terminate in the EG.

Cerebellar Fibers

In addition to comparing gyral structures of ferret and cat brains, we examined cerebellar pathways. Seed ROIs placed in the pons revealed pontocerebellar tracts that were nearly identical in both species. These bundles ran from the base of the pons to the posterior lobe of the cerebellum (Fig. 5*E*,*F*, see red circles for placement of ROIs). By placing ROIs in the dentate nucleus, we were able to observe fibers that extended throughout the cerebellum (Fig. 5*G*,*H*, see orange rectangles for placement of ROIs). Although the ferret cerebellum is more posteriorly located and occupies a smaller relative space, the branching pattern and distribution of major bundles in the anterior and posterior lobes was homologous. Fibers extending out the cerebellum exhibited similar connectivity and branching. ROIs placed in the dentate nucleus of both cats and ferrets show dentatothamalic tracts extending, through the superior peduncle, into the ventral lateral nucleus of the thalamus and the striatum (see red arrows in Fig. 5*J*, see red circles for placement of ROIs).

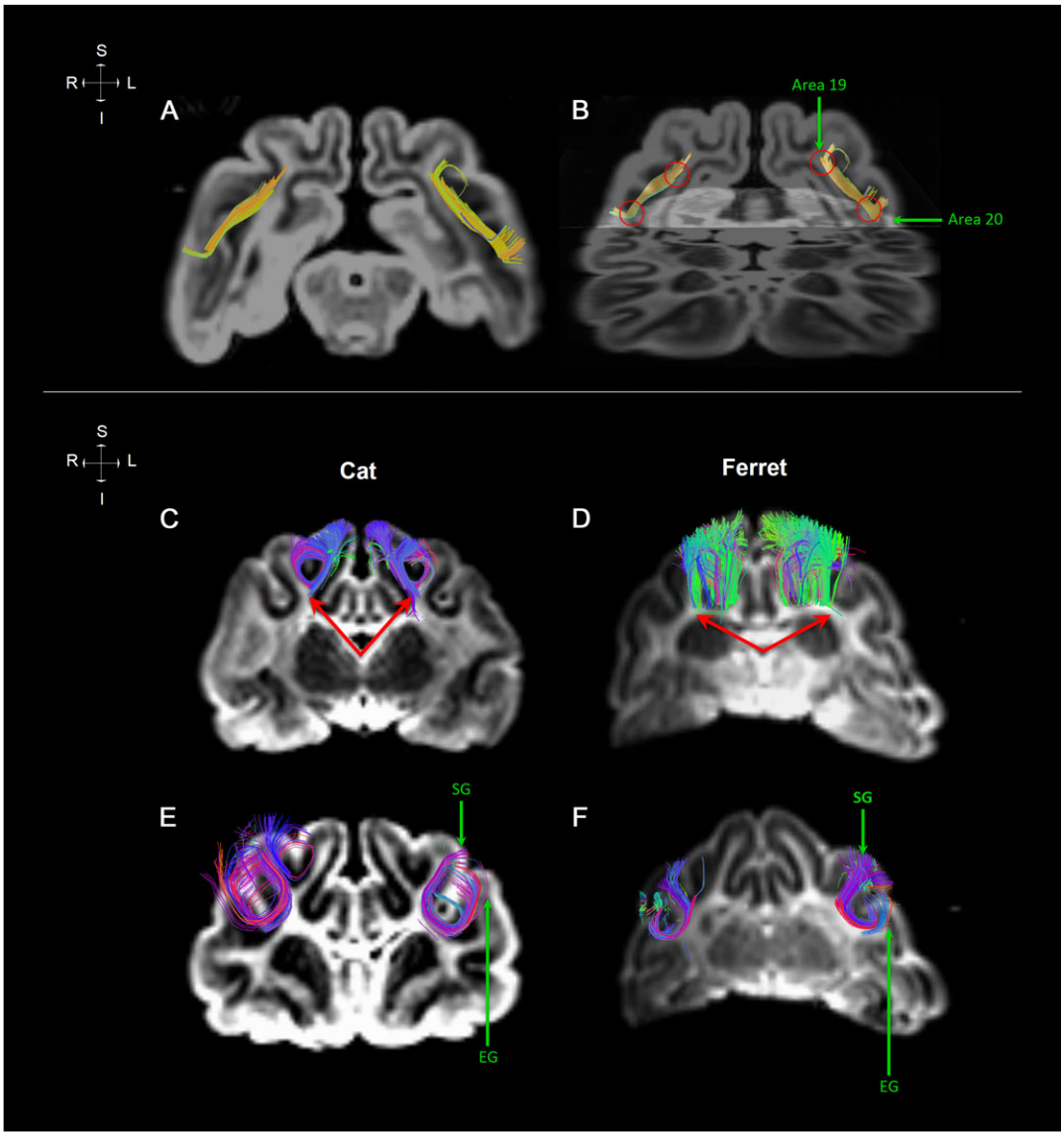

Figure 3. (*A*) and (*B*) show coronal views of associative bundles connecting areas 19 and 20 of the cat visual cortex. The lower figure shows coronal views of U-fibers extending from the lateral to the suprasylvian gyrus, (*C*) and (*D*), and the suprasylvian (SG) to the EG, (*E*) and (*F*). (*C*) and (*E*) are of a cat while (*D*) and (*F*) are of a ferret. Red arrows in (*A*) and (*B*) draw attention to the lack of lateral-suprasylvian U-fibers in ferrets. Red circles indicate placement of ROIs.

Discussion

In this study, we present a comparative DSI tractography focusing on cat and ferret white matter pathways. We successfully mapped homologous gyral structures in both cats and ferrets and were able to identify several significant differences in their connectivity. Many connectional differences between the 2 species were centered on the visual cortex. Cat brains contained many connections to the visual cortex that were either significantly different or absent in ferrets. Additional connectivity differences were found in the auditory cortices. These results indicate that, while species may share similar gyral structures, they can develop different underlying white matter connectivity.

Differences in Visual Connectivity

Among the white matter tracts mapped, one of the greatest areas of organizational and connectional difference was in the visual cortex. Cats possessed a set of associative pathways connecting visual areas 19 and 20 that were absent in ferrets. Previous lesion and cooling loop studies have shown these areas are integral to the cat's ability to recognize and discriminate patterns (Doty 1971; Sprague 1977; Lomber et al. 1996). Additional differences were found in the cingulum of both species. While the ferret cingulum remains on the midline of the brain, the cat cingulum bundle branches and extends into visual area 20 (Fig. 2). This branching pattern of the cat cingulum is consistent with previous studies at various ages (Takahashi et al. 2010) and indicates an underlying difference in the connectivity of the visual cortex. Additional connectional disparities include the longitudinal pathway running through the suprasylvian gyrus, which is typically known to connect the temporal, occipital, and parietal areas of the brain with the frontal lobe (Schmahmann et al. 2008). In cats, this pathway can be seen extending from the frontal cortex, through the parietal area, and into the visual cortex. In contrast, the ferret

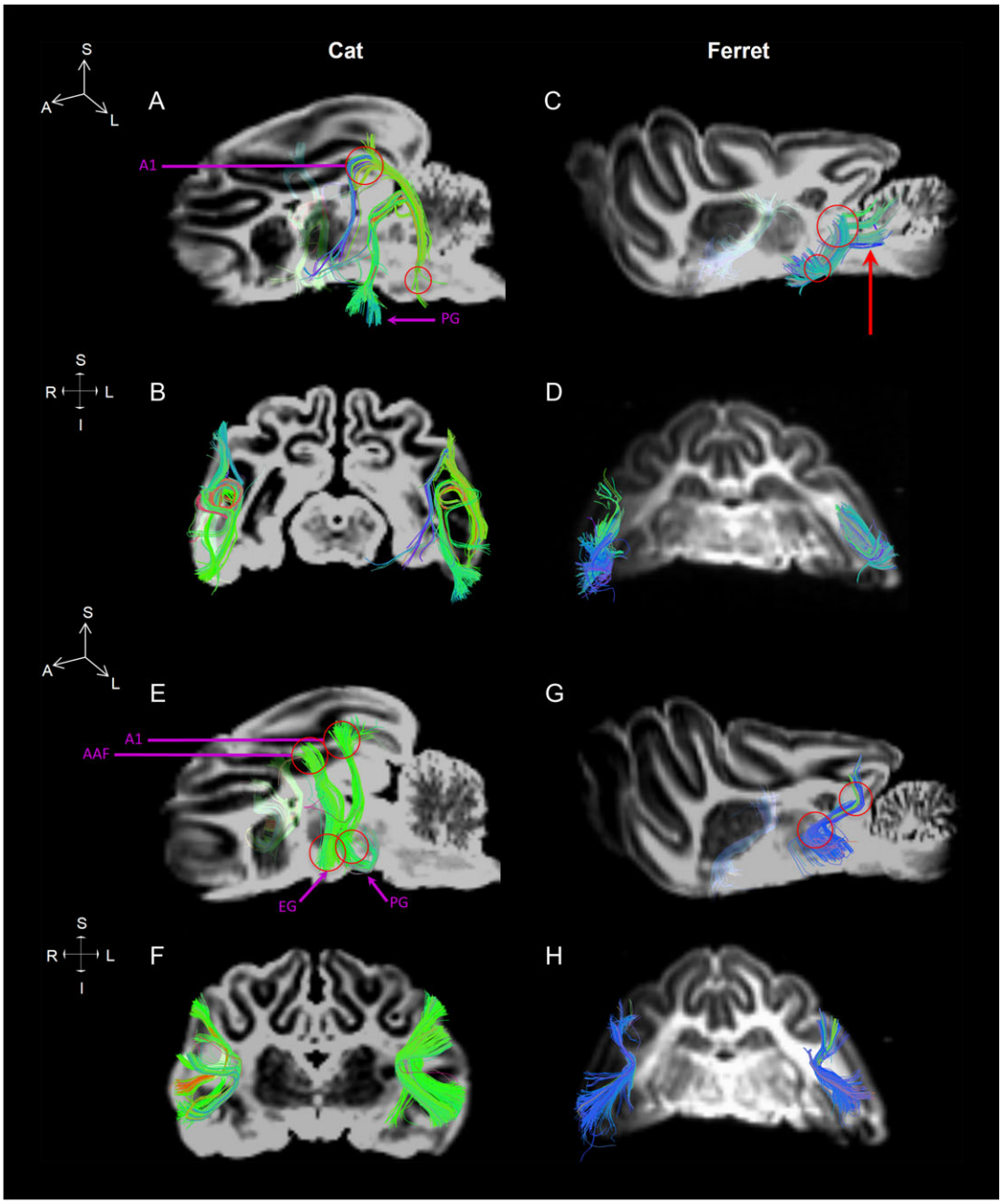

Figure 4. Oblique (*A*) and coronal (*B*) views of cortico-cortical tracts in the posterior ectosylvian gyrus of cats. (*C*) and (*D*) show oblique and coronal views of similar ROI placement in ferrets. Oblique (*E*) and coronal (*F*) views of additional cortico-cortical tracts extending from the mid-EG to the bottom of the PG of cats. (*G*) and (*H*) show oblique and coronal views of similar ROI placement in ferrets with tracts extending from the mid-EG to the lower EG. The red arrow in (*C*) shows the extension of auditory fibers in the ferret visual cortex. Red circles indicate placement of ROIs. AAF, anterior auditory field; A1, primary autditory cortex.

pathway is thinner and located more anteriorly. Additionally, the ferret pathway extends from the frontal lobe and into the sensorimotor area, failing to reach the main visual cortex as in cats (Fig. 2*E*,*F*).

The differing connectivity found in cat and ferret brains may be attributed to anatomical distinctions in their visual systems. Previous anatomical studies have shown ferrets to possess substantially larger receptive fields, more laterally placed eyes, and a stronger visual streak than cats (Stone 1978; Vitek et al. 1985; Zahs and Stryker 1985). Additional histological studies show that the distribution of ON and OFF centered cells in the LGN and the cortex differs between cats and ferrets (Sanderson 1971; Stryker and Zahs 1983; Law et al. 1988; Zahs and Stryker 1988). The LGN serves as a relay between the eyes and the primary visual cortex. If the distribution and localization of ON and OFF cells differs in the LGN between the 2 species, it is reasonable to assume differences in white matter tracts will result. The data gathered in this study appear to be consistent with these histological differences. Figure 5 shows differing connectivity between the LGN and the primary visual cortex in cats and ferrets. In cats, the thalamo-cortical fibers from the LGN are tightly bound and innervate areas on both

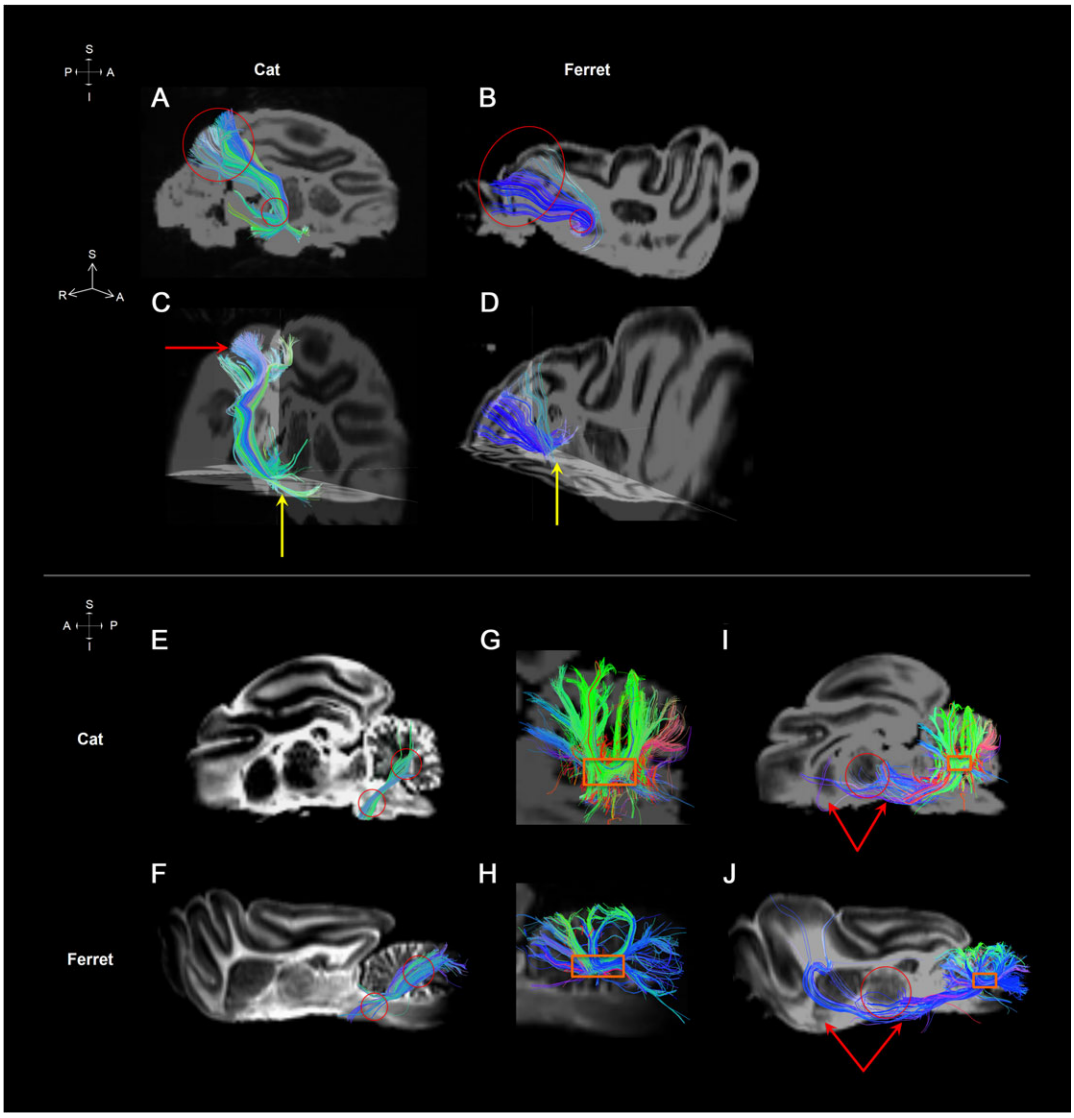

Figure 5. Sagittal and 3D views of thalamo-cortical fibers connecting the LGN and the visual cortex. (*A*) and (*B*) show a cat and (*C*) and (*D*) show a ferret. The left side of the 3D images represent the left side of the brain. The red arrow in (*C*) shows the branching fibers that innervate the suprasylvian gyrus. Yellow arrows in (*C*) and (*D*) show the differing amount of thalamic projections between cats and ferrets. Red circles indicate placement of ROIs. Cerebellar pathways. (*E*) and (*F*) show sagittal views of pontocerebellar fibers. (*G*) and (*H*) show sagittal views of fibers originating in the dentate nucleus extending throughout the cerebellum. (*I*) and (*J*) show thalamo-cerebellar fibers and additional connections extending the striatum. (*E*), (*G*), and (*I*) show a cat brain while (*F*), (*H*), and (*J*) show a ferret brain. Red arrows in (*E*) and (*F*) show both striatal and thalamic connectivity with the cerebellum, respectively. Red circles and orange rectangles show placement of ROIs.

the posterior suprasylvian and lateral gyri. In contrast, homologous white matter pathways in ferrets extend only into the lateral gyrus, despite ferrets being known to have areas of visual activity in the suprasylvian gyrus (Manger et al. 2002, 2004, 2005; Ramsay and Meredith 2004; Bizley et al. 2005).

While not directly relevant to this study, as white matter pathways were being compared across species and did not vary significantly between samples, the cortical surface morphology of the caudal descending lateral gyrus in ferrets can vary inter-individually and inter-sexually (Sawada and Watanabe 2012; Sawada et al. 2015). A future supplement to this study may include an intra-species examination of gyrification index and diffusion MR measurements across samples to determine a relationship between white matter connectivity and gyrification.

Differences in Auditory Connectivity

The temporal lobe is far larger and more expanded in cats than in ferrets. As a result, we expected connectional and organizational differences between the 2 species. The pathways discussed in Fig. 4*A* and *B* show fiber tracts along the posterior EG that runs to A1. This connectivity is integral to proper auditory functions in cats, as deactivations of non-primary auditory areas along the length of the tract have been shown to cause severe sound localization deficits (Malhotra et al. 2004, 2008; Lomber and Malhotra 2008). The fiber tracts shown in Fig. 4*C* and *D*, the result of placing ROIs in homologous locations in ferrets, differ widely from those seen in cats. While the cortico-cortical pathways observed in cats interconnected essential auditory areas, the fiber bundles shown in ferrets extend

beyond the ferret auditory cortex into ferret visual area 21. The observation of these white matter tracts is in concordance with previous tracer and electrophysiological studies that observed visual inputs in auditory areas of the ferret brain (Bizley et al. 2007). The presence of these visuo-auditory connections demonstrates further differences in visual connectivity between the 2 species.

Cerebellar Pathways

Because the cerebellum is a highly conserved portion of the brain and previous electrophysiological studies (Oscarsson 1980; Garwicz 1997) had shown similar functional organization of cerebellar lobes, we expected no significant differences in cerebellar white matter pathways. Tractography within the cerebellum yielded results consistent with this assumption. Pathways extending through the dentate nucleus innervated the anterior and posterior cerebellar lobes similarly in both species. Additional efferent connections from the cerebellum were also similar between the species. In both cats and ferrets dentatothalamic tracts extended through the thalamus and into the striatum. This connectivity is consistent with studies conducted in rats and various species of monkey (Ichinohe et al. 2000; Hoshi et al. 2005; Bostan et al. 2010), further demonstrating the conserved nature of mammalian cerebellar development.

Limitations

The axonal tension theory (Van Essen 1997) proposes that the mechanical forces necessary for cortical folding come from tension generated by axons pulling strongly interconnected brain regions together. The theory specifically suggests that short-range interregional connections that traverse sulcal walls cause gyrification, and that sulci form between regions that are not so strongly connected. While this study examines various types of white matter connectivity between homologous gyri, the majority of the observed tracts are not implicated in the tension theory of cortical folding, limiting possible conclusions on the theory. While an absence of U-fibers in a species represents a significant difference in connectivity, it is important to note that U-fibers do not play a major role in the traditional tension model of gyrification. A recent extension to the tension theory (Herculano-Houzel et al. 2010), stating axonal tension caused by increasing subcortical white matter connectivity, pulls down on the adjacent cortical gray matter to generate folding, suggests a possible implication of U-fibers in gyrification; however, because of the qualitative nature of this study it is difficult to assess their direct impact. Furthermore, it is important to recognize the presence of additional types of white matter pathways in the area and their potential collective role in gyrification. Recent studies examining the axonal tension theory have found that, while axonal tension plays a role during brain development, it is not the primary cause of cortical folding (Xu et al. 2010; Rash et al. 2013). Alternative mechanisms, such as growth of large axonal tracts (Goldman-Rakic and Rakic 1984), in late neurogenesis even postnatally in some species (Ferrer et al. 1988; Sawada et al. 2012; Schmidt et al. 2012) suggest multiple mechanisms may be responsible for secondary and tertiary gyrification.

Based on our results, we see that it is possible that similar gyral structures can have different underlying white matter connectivity in different species. While we observed differing connectivity in adult brains, it is important to recognize the possibility of developmental pruning. It is possible that cat and ferret brains had similar white matter tracts during development, but subsequent pruning during maturation led to the observed differences. Because this study intended only to examine adult cats and ferrets, with the data available, we were unable to draw conclusions on the white matter tracts during early gyral development. A comparison of embryological data of cat/ferret and/or other species will help in understanding whether gyral connectivity is inherently different between the 2 species or is a product of axonal pruning during development, while also helping to further investigate the causality of the relationships between gyrification and fiber development.

Funding

The Eunice Shriver Kennedy National Institute of Child Health and Development (NICHD) (R01HD078561); National Institute of Neurological Disorders and Stroke (NINDS) (R03NS091587) (ET). This research was carried out in part at the Athinoula A. Martinos Center for Biomedical Imaging at the Massachusetts General Hospital, using resources provided by the Center for Functional Neuroimaging Technologies, P41RR14075, a P41 Regional Resource supported by the Biomedical Technology Program of the National Center for Research Resources (NCRR), National Institutes of Health. This work also involved the use of instrumentation supported by the NCRR Shared Instrumentation Grant Program (S10RR023401, S10RR019307, and S10RR023043) and a High-End Instrumentation Grant Program (S10RR016811).

Notes

We thank Kenichi Ohki for providing the specimens with technical assistance, and Guangping Dai for technical assistance. *Conflict of Interest*: None declared.

References

Barbas H, Rempel-Clower N. 1997. Cortical structure predicts the pattern of corticocortical connections. Cereb Cortex. 7: 635–646.

Barnette AR, Neil JJ, Kroenke CD, Griffith JL, Epstein AA, Bayly PV, Knutsen AK, Inder TE. 2009. Characterization of brain development in the ferret via MRI. Pediatr Res. 66:80–84.

Basser PJ, Mattiello J, LeBihan D. 1994. Estimation of the effective self-diffusion tensor from the NMR spin echo. J Magn Reson B. 103:247–254.

Basser PJ, Pajevic S, Pierpaoli C, Duda J, Aldroubi A. 2000. In vivo fiber tractography using DT-MRI data. Magn Reson Med. 44: 625–632.

Bizley JK, Nodal FR, Bajo VM, Nelken I, King AJ. 2007. Physiological and anatomical evidence for multisensory interactions in auditory cortex. Cereb Cortex. 17:2172–2189.

Bizley JK, Nodal FR, Nelken I, King AJ. 2005. Functional organization of ferret auditory cortex. Cereb Cortex. 15:1637–1653.

Bock AS, Olavarria JF, Leigland LA, Taber EN, Jespersen SN, Kroenke CD. 2010. Diffusion tensor imaging detects early cerebral cortex abnormalities in neuronal architecture induced by bilateral neonatal enucleation: an experimental model in the ferret. Front Syst Neurosci. 4:149.

Bostan AC, Dum RP, Strick PL. 2010. The basal ganglia communicate with the cerebellum. Proc Natl Acad Sci USA. 107: 8452–8456.

Callaghan PT. 1991. Principles of nuclear magnetic resonance microscopy. New York (NY): Oxford University Press.

Callaway EM, Katz LC. 1990. Emergence and refinement of clustered horizontal connections in cat striate cortex. J Neurosci. 10:1134–1153.

Catani M, Howard RJ, Pajevic S, Jones DK. 2002. Virtual in vivo interactive dissection of white matter fasciculi in the human brain. NeuroImage. 17:77–94.

Cavagna P, Menotti A, Stanyon R. 2000. Genomic homology of the domestic ferret with cats and humans. Mamm Genome. 11:866–870.

Cellerini M, Konze A, Caracchini G, Santoni M, Dal Pozzo G. 1997. Magnetic resonance imaging of cerebral associative white matter bundles employing fast-scan techniques. Acta Anat (Basel). 158:215–221.

Conturo TE, Lori NF, Cull TS, Akbudak E, Snyder AZ, Shimony JS, McKinstry RC, Burton H, Raichle ME. 1999. Tracking neuronal fiber pathways in the living human brain. Proc Natl Acad Sci USA. 96:10422–10427.

Doty RW. 1971. Survival of pattern vision after removal of striate cortex in the adult cat. J Comp Neurol. 143:341–369.

Ferrer I, Hernåndez-Marti M, Bernet E, Galofré E. 1988. Formation and growth of the cerebral convolutions. I. Postnatal development of the median-suprasylvian gyrus and adjoining sulci in the cat. J Anat. 160:89–100.

Foxworthy WA, Meredith MA. 2011. An examination of somatosensory area SIII in ferret cortex. Somatosens Mot Res. 28: 1–10.

Garwicz M. 1997. Sagittal zonal organization of climbing fibre input to the cerebellar anterior lobe of the ferret. Exp Brain Res. 117:389–398.

Goldman-Rakic PS, Rakic P. 1984. Experimental modification of gyral patterns. In: Geschwind N, Galaburda A, editors. Cerebral dominance: Biological Foundations. Cambridge (MA): Harvard University Press. p. 179–192.

Hagmann P, Cammoun L, Gigandet X, Meuli R, Honey CJ, Wedeen VJ, Sporns O. 2008. Mapping the structural core of human cerebral cortex. PLoS Biol. 6:e159.

Herculano-Houzel S, Mota B, Wong P, Kaas J. 2010. Connectivity-driven white matter scaling and folding in primate cerebral cortex. Proc Natl Acad Sci USA. 107(44):19008–19013.

Hilgetag CC, Barbas H. 2005. Developmental mechanics of the primate cerebral cortex. Anat Embryol. 210:411–417.

Hofman MA. 2014. Evolution of the human brain: when bigger is better. Front Neuroanat. 8:1–12.

Hoshi E, Tremblay L, Féger J, Carras PL, Strick PL. 2005. The cerebellum communicates with the basal ganglia. Nat Neurosci. 8:1491–1493.

Ichinohe N, Mori F, Shoumura K. 2000. Di-synaptic projection from the lateral cerebellar nucleas to the laterodorsal part of the striatum via the central lateral nucleus of the thalamus in the rat. Brain Res. 880:191–197.

Innocenti GM, Manger PR, Masiello I, Colin I, Tettoni L. 2002. Architecture and callosal connections of visual areas 17, 18, 19 and 21 in the ferret (Mustela putorius). Cereb Cortex. 12: 411–422.

Issa NP, Trachtenberg JT, Chapman B, Zahs KR, Stryker MP. 1999. The critical period for ocular dominance plasticity in the Ferret's visual cortex. J Neurosci. 19:6965–6978.

Jones DK, Simmons A, Williams SC, Horsfield MA. 1999. Non-invasive assessment of axonal fiber connectivity in the human brain via diffusion tensor MRI. Magn Reson Med. 42: 37–41.

Kim DS, Kim M, Ronen I, Formisano E, Kim KH, Ugurbil K, Mori S, Goebel R. 2003. In vivo mapping of functional domains and axonal connectivity in cat visual cortex using magnetic resonance imaging. Magn Reson Imaging. 21:1131–1140.

Kroenke CD, Taber EN, Leigland LA, Knutsen AK, Bayly PV. 2009. Regional patterns of cerebral cortical differentiation determined by diffusion tensor MRI. Cereb Cortex. 19: 2916–2929.

Law MI, Zahs KR, Stryker MP. 1988. Organization of primary visual cortex (area 17) in the ferret. J Comp Neurol. 278:157–180.

Le Bihan D, Mangin JF, Poupon C, Clark CA, Pappata S, Molko N, Chabriat H. 2001. Diffusion tensor imaging: concepts and applications. J Magn Reson Imaging. 13:534–546.

Lin CP, Wedeen VJ, Chen JH, Yao C, Tseng WY. 2003. Validation of diffusion spectrum magnetic resonance imaging with manganese-enhanced rat optic tracts and ex vivo phantoms. Neuroimage. 19:482–495.

Lomber SG, Malhotra S. 2008. Double dissociation of 'what' and 'where' processing in auditory cortex. Nat Neurosci. 11: 609–616.

Lomber SG, Payne BR, Cornwell P. 1996. Leaning and recall of form discriminations during reversible cooling deactivations of ventral-posterior suprasylvian cortex in the cat. Proc Natl Acad Sci USA. 93:1654–1658.

Makris N, Worth AJ, Sorensen AG, Papadimitriou GM, Wu O, Reese TG, Wedeen VJ, Davis TL, Stakes JW, Caviness VS, et al. 1997. Morphometry of in vivo human white matter association pathways with diffusion-weighted magnetic resonance imaging. Ann Neurol. 42:951–962.

Malhotra S, Hall AJ, Lomber SG. 2004. Cortical control of sound localization in the cat: unilateral cooling deactivation of 19 cerebral areas. J Neurophysiol. 92:1625–1643.

Malhotra S, Stecker CG, Middlebrooks JC, Lomber SG. 2008. Sound localization deficits during reversible deactivation of primary auditory cortex and/or the dorsal zone. J Neurophysiol. 99:1628–1642.

Manger PR, Engler G, Moll CK, Engel AK. 2005. The anterior ectosylvian visual area of the ferret: a homologue for an enigmatic visual cortical area of the cat? J Neurosci. 22:706–714.

Manger PR, Masiello I, Innocenti GM. 2002. Areal organization of the posterior parietal cortex of the ferret (Mustela putorius). Cereb Cortex. 12:1280–1297.

Manger PR, Nakamura H, Valentiniene S, Innocenti GM. 2004. Visual areas in the temporal cortex of the ferret (Mustela putorius). Cereb Cortex. 14:676–689.

Markham JA, Greenough WT. 2004. Experience-driven brain plasticity: beyond the synapse. Neuron Glia Biol. 1:351–363.

Mayer J, Erdman SE, Fox JG. 2014. Diseases of the hematopoietic system, in biology and diseases of the ferret. Ames (IA): John Wiley & Sons, Inc.

Mori S, Crain BJ, Chacko VP, van Zijl PC. 1999. Three-dimensional tracking of axonal projections in the brain by magnetic resonance imaging. Ann Neurol. 45:265–269.

Olavarria JF, Van Sluyters RC. 1995. Overall pattern of callosal connections in visual cortex of normal and enucleated cats. J Comp Neurol. 363:161–176.

Oscarsson O. 1980. Functional organization of olivary projection to the cerebellar anterior lobe. In: Courville J, de Montigny C, Lamarre Y, editors. The inferior olivary nucleus: anatomy and physiology. New York (NY): Raven Press. p. 279–289.

Pierpaoli C, Jezzard P, Basser PJ, Barnett A, Di Chiro G. 1996. Diffusion tensor MR imaging of the human brain. Radiology. 201:637–648.

Ramsay AM, Meredith MA. 2004. Multiple sensory afferents to ferret pseudosylvian sulcal cortex. Neuroreport. 15:461–465.

Rash BG, Tomashi SH, Lim D, Suh CY, Vaccarino FM. 2013. Cortical gyrification induced by fibroblast growth factor 2 in the mouse brain. J Neurosci. 33:10802–10814.

Rosenquist AC. 1985. Connections of visual cortical areas in the cat. In: Peters A, Jones EG, editors. Cerebral Cortex. Vol. 3. New York (NY): Plenum Press. p. 81–117.

Sanderson KJ. 1971. The projection of the visual field to the lateral geniculate and medial interlaminar nuclei in the cat. J Comp Neurol. 143:101–117.

Sawada K, Fukunishi K, Kashima M, Saito S, Sakata-Haga H, Aoki I, Fukui Y. 2012. Fetal gyrification in cynomologus monkeys: a concept of developmental stages in gyrification. Anat Rec. 295:1065–1074.

Sawada K, Horiuchi-Hirose M, Saito S, Aoki I. 2015. Sexual dimorphism of sulcal morphology of the ferret cerebrum revealed by MRI-based sulcal surface morphometry. Front Neuroanat. 9:55.

Sawada K, Watanabe M. 2012. Development of cerebral sulci and gyri in ferrets (Mustela putorius). Congenit Anom. 52:168–175.

Schmahmann JD, Smith EE, Eichler FS, Filley CM. 2008. Cerebral white matter: neuroanatomy, clinical neurology, and neurobehavioral correlates. Ann NY Acad Sci. 1142:266–309.

Schmidt MJ, Amort K, Kramer M. 2012. Postnatal development of the cerebral gyrification in the canine brain. Vet Radiol Ultrasound. 53:643–649.

Sprague JM. 1977. Visual cortex areas mediating form discrimination in the cat. J Comp Neurol. 172:441–488.

Stone J. 1978. The number and distribution of ganglion cells in the cat's retina. J Comp Neurol. 180:753–772.

Stryker MP, Zahs KR. 1983. ON and OFF sublaminae in the lateral geniculate nucleus of the ferret. J Neurosci. 3:1943–1951.

Takahashi E, Dai G, Wang R, Ohki K, Rosen GD, Galaburda AM, Grant PE, Wedeen VJ. 2010. Development of cerebral fiber pathways in cats revealed by diffusion spectrum imaging. Neuroimage. 49:1231–1240.

Takahashi E, Ohki K, Kim DS. 2007. Diffusion tensor studies dissociated two fronto-temporal pathways in the human memory system. Neuroimage. 34:827–838.

Takahashi E, Ohki K, Kim DS. 2008. Dissociated pathways for successful memory retrieval from the human parietal cortex: anatomical and functional connectivity analyses. Cereb Cortex. 18:1771–1778.

Van Essen DC. 1997. A tension-based theory of morphogenesis and compact wiring in the central nervous system. Nature. 385:313–318.

Vitek DJ, Schall JD, Leventhal AG. 1985. Morphology, central projections and dendritic field orientation of retinal ganglion cells in the ferret. J Comp Neurol. 241:1–11.

Wedeen VJ, Hagmann P, Tseng WY, Reese TG, Weisskoff RM. 2005. Mapping complex tissue architecture with diffusion spectrum magnetic resonance imaging. Magn Reson Med. 54:1377–1386.

Wedeen VJ, Wang RP, Schmahmann JD, Benner T, Tseng WY, Dai G, Pandya DN, Hagmann P, D'Arceuil H, de Crespigny AJ. 2008. Diffusion spectrum magnetic resonance imaging (DSI) tractography of crossing fibers. Neuroimage. 41: 1267–1277.

Xu G, Knutsen AK, Dikranian K, Kroenke CD, Bayly PV, Taber LA. 2010. Axons pull on the brain, but tension does not drive cortical folding. J Biomech Eng. 132:071013.

Zahs KR, Stryker MP. 1985. The projection of the visual field onto the lateral geniculate nucleus of the ferret. J Comp Neurol. 241:210–224.

Zahs KR, Stryker MP. 1988. Segregation of ON and OFF afferents to ferret visual cortex. J Neurophysiol. 59:1410–1429.